Determination of Adsorption Isotherms of Hydroxide and Deuteroxide on Pt−Ir Alloy in LiOH Solutions Using the Phase-Shift Method and Correlation Constants

Jinyoung Chun,[†] Nam Y. Kim,[‡] and Jang H. Chun*,[‡]

Department of Chemical Engineering, Pohang University of Science and Technology, Pohang, Kyungbuk 790-784, Republic of Korea, and Department of Electronic Engineering, Kwangwoon University, Seoul 139-701, Republic of Korea

The phase-shift method and correlation constants, that is, unique electrochemical impedance spectroscopy techniques for studying the linear relationship between the behavior ($-\varphi$ vs E) of the phase shift ($90° \geq -\varphi \geq 0°$) for the optimum intermediate frequency and that (θ vs E) of the fractional surface coverage ($0 \leq \theta \leq 1$) of intermediates for sequential reactions, are proposed and verified to determine the Frumkin, Langmuir, and Temkin adsorption isotherms and related electrode kinetic and thermodynamic parameters. On Pt−Ir (90:10 % (by weight)) alloy in 0.1 M LiOH (H_2O) and 0.1 M LiOH (D_2O) solutions, the Frumkin and Temkin adsorption isotherms (θ vs E), equilibrium constants (K), interaction parameters (g), rates (r) of change of the standard Gibbs energies of hydroxide (OH) and hydroxide and deuteroxide (OH, OD) with θ, and standard Gibbs energies (ΔG_θ^0) of OH and (OH, OD) are determined and compared using the phase-shift method and correlation constants. Depending on θ ($0 \leq \theta \leq 1$), the value of K for OH is approximately 1.4 to 11.5 times greater than that for (OH, OD). The OD effect on the adsorption of (OH, OD) on the Pt−Ir alloy in 0.1 M LiOH (D_2O) solution is not negligible, especially when E is high and $\theta \approx 1$. Both the values of K for OH and (OH, OD) decrease with increasing E and θ. A lateral repulsion ($g > 0$) interaction between the adsorbed OH or (OH, OD) species appears.

Introduction

The adsorption of H for the cathodic H_2 evolution reaction (HER) and OH for the anodic O_2 evolution reaction (OER) on noble metals (alloys) in aqueous solutions has been extensively studied in electrochemistry, electrode kinetics, surface science, and so forth.[1−3] It is preferable to consider the Frumkin, Langmuir, and Temkin adsorption isotherms for H and OH rather than equations of the electrode kinetics and thermodynamics for H and OH, because these adsorption isotherms are associated more directly with the atomic mechanism of H and OH.[4] However, there is not much reliable information on the Frumkin, Langmuir, and Temkin adsorption isotherms of OH and hydroxide and deuteroxide (OH, OD) for the anodic OER and related electrode kinetic and thermodynamic parameters of noble metals (alloys) in alkaline ordinary water (H_2O) and heavy water (D_2O) solutions. Thus, there is a technological need for a simple, accurate, and reliable method to determine the Frumkin, Langmuir, and Temkin adsorption isotherms for characterizing the adsorption of OH and (OH, OD) for the anodic OER on the noble metals (alloys) in alkaline H_2O and D_2O solutions.

Many scientific phenomena have been interpreted by their behavior rather than by their nature. For example, the duality of light and electrons, that is, the wave and particle behaviors, is well-known in science and has been applied in engineering. Note that these wave and particle behaviors are not contradictory to each other but complementary. The phase-shift method and correlation constants are unique electrochemical impedance spectroscopy techniques for studying the linear relationship between the behavior ($-\varphi$ vs E) of the phase shift ($90° \geq -\varphi \geq 0°$) for the optimum intermediate frequency and that (θ vs E) of the fractional surface coverage ($0 \leq \theta \leq 1$) of intermediates (H, OH, etc.) for sequential reactions (HER, OER, etc.) on noble and highly corrosion-resistant metals (alloys) in aqueous solutions.[5−20] The behavior (θ vs E) of the fractional surface coverage ($0 \leq \theta \leq 1$) is well-known as the Frumkin or the Langmuir adsorption isotherm.[1−4]

New ideas or techniques must be rigorously tested, especially when they are unique, but only with pure logic and objectivity and through scientific methods and procedures. However, the objections to the phase-shift method in the comments[21−23] do not fulfill these criteria. These objections are substantially attributed to the confusion and misunderstanding about the phase-shift method itself.[20,24,25] Note especially that all the objections to the phase-shift method in the comments[21,23] are attributed to the confusion and misunderstanding about the applicability of related equations for intermediate frequencies and a unique feature of the Faradaic resistances for the recombination steps.[20,26]

In practice, the numerical calculation or simulation of equivalent circuit impedances of metals (alloys) in solutions is very difficult or impossible due to the superposition of various effects, that is, relaxation time effects, real surface area problems, surface absorption and diffusion processes, inhomogeneous and lateral interaction effects, oxide layer formations, specific adsorption effects, and so forth. However, it is simply determined or measured by frequency analyzers, that is, instruments or tools. Note that the phase-shift method is a useful and efficient tool for determining the Frumkin, Langmuir, and Temkin adsorption isotherms. The validity and correctness of the phase-shift method should be discussed on the basis of simulations with a single equation for $-\varphi$ versus θ as a function

* To whom correspondence should be addressed. E-mail: jhchun@kw.ac.kr. Fax: +82-2-942-5235. Tel.: +82-2-940-5116.
[†] Pohang University of Science and Technology.
[‡] Kwangwoon University.

10.1021/je100328d
Published on Web 08/05/2010

of potential (E) and frequency (f) or relevant experimental results which are obtained using other conventional methods. However, the single equation for ($-\varphi$ vs θ) as a function of E and f has never been derived or discussed on the basis of relevant experimental results.[21−23] The simulations on the phase-shift method without this single equation are basically meaningless or in vain.[20,24−26] Note that this problem has been experimentally and consistently solved using the phase-shift method for determining adsorption isotherms.

In this paper, we represent and compare the Frumkin and Temkin adsorption isotherms of OH and (OH, OD) and related electrode kinetic and thermodynamic parameters of the Pt−Ir (90:10 % (by weight)) alloy in 0.1 M LiOH (H_2O) and 0.1 M LiOH (D_2O) solutions using the phase-shift method and correlation constants. In contrast to a negative value of the interaction parameter for the Frumkin adsorption isotherms of H on Pt, Ir, and Pt−Ir alloys,[17] a positive value of the interaction parameter for the Frumkin adsorption isotherms of OH and (OH, OD) on the Pt−Ir alloy in 0.1 M LiOH (H_2O) and 0.1 M LiOH (D_2O) solutions is determined. The OD effect on the adsorption of (OH, OD) for the anodic OER on noble metals (alloys) in alkaline D_2O solutions has never been discussed on the basis of the Frumkin and Temkin adsorption isotherms elsewhere. This paper is the supplement to previously published papers.[15,20]

Experimental Section

Preparations. Taking into account the OH^- and OD^- concentrations and effects of the diffuse double layer and pOH,[27] 0.1 M LiOH (H_2O) and 0.1 M LiOH (D_2O) alkaline solutions were prepared from LiOH (Alfa Aesar, purity: 99.995 %) with purified water (H_2O, resistivity: > 18 MΩ·cm) obtained from a Millipore system and heavy water (D_2O, Alfa Aesar, purity: 99.8 %), respectively. The values of pOH and p(OH, OD) of 0.1 M LiOH (H_2O) and 0.1 M LiOH (D_2O) solutions are approximately 1.26 and 0.96, respectively. These solutions were deaerated with 99.999 % purified nitrogen gas for 20 min before the experiments. A standard three-electrode configuration was employed. A saturated calomel electrode (SCE) was used as the standard reference electrode. A platinum−iridium alloy wire (Johnson Matthey, Pt:Ir; 90:10 % (by weight), 1.5 mm diameter, estimated surface area: ca. 1.19 cm^2) was used as the working electrode. A platinum wire (Johnson Matthey, purity: 99.95 %, 1.5 mm diameter, estimated surface area: ca. 2.01 cm^2) was used as the counter electrode. The Pt−Ir alloy working electrode was prepared by flame cleaning and then quenched and cooled in Millipore Milli-Q water and in air, sequentially.

Measurements. A cyclic voltammetry (CV) technique was used to achieve steady states on the Pt−Ir alloy in 0.1 M LiOH (H_2O) and 0.1 M LiOH (D_2O) solutions, respectively. The CV experiments were conducted for 50 cycles, with a scan rate of 200 $mV \cdot s^{-1}$ and a scan potential of (0 to 1.0) V versus the SCE on the Pt−Ir alloy in 0.1 M LiOH (H_2O) and 0.1 M LiOH (D_2O) solutions, respectively. After the CV experiments, an electrochemical impedance spectroscopy (EIS) technique was used to study the linear relationship between the behavior ($-\varphi$ vs E) of the phase shift ($90° \geq -\varphi \geq 0°$) for the optimum intermediate frequency and that (θ vs E) of the fractional surface coverage ($0 \leq \theta \leq 1$) on the Pt−Ir alloy in 0.1 M LiOH (H_2O) and 0.1 M LiOH (D_2O) solutions, respectively. The EIS experiments were conducted at scan frequencies of (10^4 to 0.1) Hz for high- and intermediate-frequency responses, a single sine wave, an alternating current (ac) amplitude of 5 mV, and a direct current (dc) potential of (0 to 1.0) V versus the SCE on the Pt−Ir alloy in 0.1 M LiOH (H_2O) and 0.1 M LiOH (D_2O) solutions, respectively.

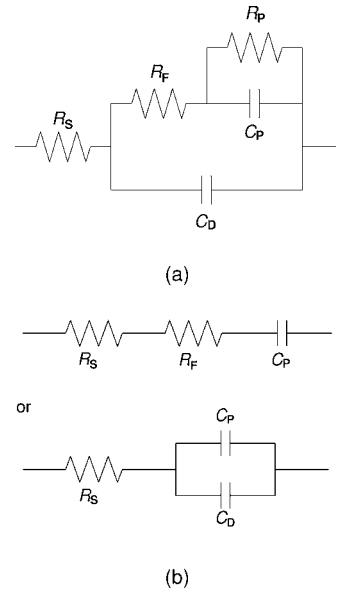

Figure 1. (a) Experimentally proposed equivalent circuit for the phase-shift method and (b) simplified equivalent circuit for intermediate-frequency responses. Equivalent circuit elements shown in Figure 1a are defined in this work.

The CV experiments were performed using an EG & G PAR model 273A potentiostat controlled with the PAR model 270 software package. The EIS experiments were performed using the same apparatus in conjunction with a Schlumberger SI 1255 HF Frequency Response Analyzer controlled with the PAR model 398 software package. To obtain comparable and reproducible results, all measurements were carried out using the same preparations, procedures, and conditions at room temperature. The international sign convention is used; that is, anodic currents and phase shifts or angles are taken as positive and negative, respectively. All potentials are given in the standard hydrogen electrode (SHE) scale. The Gaussian and adsorption isotherm analyses were carried out using the Excel and Origin software packages.

Results and Discussion

Theoretical and Experimental Backgrounds of the Phase-Shift Method. The equivalent circuit for the adsorption of OH and (OH, OD) for the anodic OER on the Pt−Ir alloy in 0.1 M LiOH (H_2O) and 0.1 M LiOH (D_2O) solutions can be expressed as shown in Figure 1a.[28−30] Taking into account the superposition of various effects (relaxation time effects, real surface area problems, surface absorption and diffusion processes, inhomogeneous and lateral interaction effects, oxide layer formations, specific adsorption effects, etc.) that are inevitable under the experimental measurements, we define the equivalent circuit elements. In Figure 1a, R_S is the real solution resistance; R_F is the real resistance due to the Faradaic resistance (R_ϕ) for the discharge step and superposition of various effects; R_P is the real resistance due to the Faradaic resistance (R_R) for the recombination step and superposition of various effects; C_P is the real capacitance due to the adsorption pseudocapacitance (C_ϕ) and superposition of various effects; and C_D is the real double-layer capacitance. Correspondingly, both R_F and C_P are not constant but dependent on E and θ and can be measured. Note that both R_ϕ and C_ϕ are not constant but dependent on E and θ and cannot be measured.

The numerical derivation of C_ϕ from the Frumkin and Langmuir adsorption isotherms (θ vs E) is described elsewhere,

and R_ϕ depends on C_ϕ.[28,29] A unique feature of R_ϕ and C_ϕ attaining maximum values at $\theta \approx 0.5$ and intermediate E, decreasing symmetrically with E at other values of θ, and approaching minimum values at $\theta \approx 0$ and low E and $\theta \approx 1$ and high E is well-known in interfacial electrochemistry, electrode kinetics, and EIS.[1−3,28−30] The unique feature and combination of R_ϕ and C_ϕ versus E imply that the normalized change rate of $-\varphi$ versus E, that is, $\Delta(-\varphi)/\Delta E$, corresponds to that of θ versus E, that is, $\Delta\theta/\Delta E$, and vice versa. Both $\Delta(-\varphi)/\Delta E$ and $\Delta\theta/\Delta E$ are maximized at $\theta \approx 0.5$ and intermediate E, decrease symmetrically with E at other values of θ, and are minimized at $\theta \approx 0$ and low E and $\theta \approx 1$ and high E. Note that this is not a mere coincidence but a unique feature of the Frumkin and Langmuir adsorption isotherms. The linear relationship and Gaussian profile between ($-\varphi$ vs E) or $\Delta(-\varphi)/\Delta E$ and (θ vs E) or $\Delta\theta/\Delta E$ most clearly appear at the optimum intermediate frequency (f_o). The determination of f_o is experimentally and graphically evaluated on the basis of $\Delta(-\varphi)/\Delta E$ and $\Delta\theta/\Delta E$ for intermediate and other frequencies (see Figures 4 to 7). The importance of f_o is described elsewhere.[16] These aspects are the essential nature of the phase-shift method for determining the Frumkin, Langmuir, and Temkin adsorption isotherms.

The frequency responses of the equivalent circuit for all f shown in Figure 1a are essential for understanding the unique feature and combination of R_ϕ and C_ϕ versus E, that is, the linear relationship and Gaussian profile between ($-\varphi$ vs E) or $\Delta(-\varphi)/\Delta E$ and (θ vs E) or $\Delta\theta/\Delta E$, for f_o. At very low frequencies, the equivalent circuit for all f shown in Figure 1a can be expressed as a series circuit of R_S, R_F, and R_P. At very high frequencies, the equivalent circuit for all f shown in Figure 1a can be expressed as a series circuit of R_S and C_D. At intermediate frequencies, one finds regions in which the equivalent circuit for all f shown in Figure 1a behaves as a series circuit of R_S, R_F, and C_P or a series and parallel circuit of R_S, C_P, and C_D as shown in Figure 1b.[28,29] However, note that the simplified equivalent circuit shown in Figure 1b does not represent the change of the anodic OER itself but only the intermediate-frequency response.

In Figure 1b, the impedance (Z) and phase shift ($-\varphi$) for intermediate frequencies are given by[20]

$$Z = (R_S + R_F) - j/\omega C_P \quad (1a)$$

$$-\varphi = \arctan[1/\omega(R_S + R_F)C_P] \quad (1b)$$

or

$$Z = R_S - j/\omega(C_P + C_D) \quad (2a)$$

$$-\varphi = \arctan[1/\omega R_S(C_P + C_D)] \quad (2b)$$

$$R_P \gg 1/\omega C_P \text{ and } (R_S + R_F) \quad (3)$$

where j is an operator and is equal to the square root of -1, that is, $j^2 = -1$; ω ($= 2\pi f$) is the angular frequency; and f is the frequency. In our previously published papers, only eq 1 is used with a footnote; that is, C_P practically includes C_D (see Tables 1 and 2 in ref 15, Table 1 in ref 14, etc.). Both eqs 1 and 2 show that the effect of R_P on $-\varphi$ for intermediate frequencies is negligible. These aspects are completely overlooked, confused, and misunderstood in the comments on the phase-shift method by Horvat−Radosevic, Kvastek, and Lasia.[21−23] Correspondingly, all of the simulations on the phase-shift method using eq 1, which appears in the comments (C_P does not include C_D),[21−23] are basically invalid or wrong. All of the analyses of the effect of R_P on $-\varphi$ for intermediate frequencies are also invalid or wrong.[20,26]

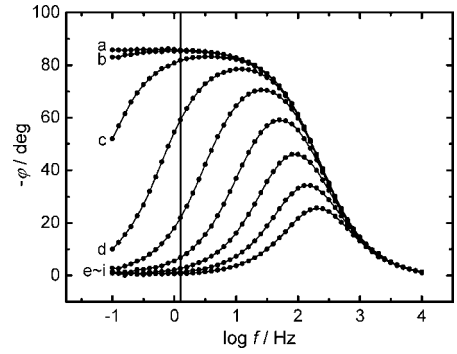

Figure 2. Comparison of the phase-shift curves ($-\varphi$ vs log f) for different potentials (E) on the Pt−Ir alloy in 0.1 M LiOH (H_2O) solution. ●, Measured value. Vertical solid line indicates 1.259 Hz; single sine wave; scan frequency, (10^4 to 0.1) Hz; ac amplitude, 5 mV; dc potential: (a) 0.641 V, (b) 0.691 V, (c) 0.741 V, (d) 0.791 V, (e) 0.841 V, (f) 0.891 V, (g) 0.941 V, (h) 0.991 V, and (i) 1.041 V versus SHE.

The following limitations and conditions of the equivalent circuit elements for f_o are summarized on the basis of the experimental data.[5−20] Both R_S and C_D are not constant. At $\theta \approx 0$, $R_S > R_F$ and $C_D > C_P$, and vice versa, and so forth. For a wide range of θ, that is, $0.2 < \theta < 0.8$, $R_F \gg R_S$ or $R_F > R_S$ and $C_P \gg C_D$ or $C_P > C_D$, and so forth. At $\theta \approx 1$, $R_S > R_F$ or $R_S < R_F$ and $C_P \gg C_D$. The measured $-\varphi$ for f_o depends on E and θ. In contrast to numerical calculations or analyses, these limitations and conditions for eq 1 or 2 are not considered for the phase-shift method, because all of the measured $-\varphi$ for intermediate frequencies include (R_S, R_F) and (C_P, C_D). Correspondingly, the measured $-\varphi$ for f_o is valid and correct regardless of the applicability of eq 1 or 2 and related limitations and conditions (see Supplementary Tables 1 and 2 in Supporting Information). This is the reason why the phase-shift method is the most useful and effective way to determine adsorption isotherms.

The unique feature and combination of (R_S, R_F) and (C_P, C_D) are equivalent to those of R_ϕ and C_ϕ. This is attributed to the reciprocal property of R_F and C_P. It suggests that only the polar form of the equivalent circuit impedance, that is, $-\varphi$ described in eq 1b or 2b, is useful and effective to study the linear relationship between the behavior ($-\varphi$ vs E) of $-\varphi$ ($90° \geq -\varphi \geq 0°$) for f_o and that (θ vs E) of θ ($0 \leq \theta \leq 1$). Note that the phase-shift method for determining adsorption isotherms is proposed and verified on the basis of the phase-shift curves ($-\varphi$ vs log f) for different E (see Figures 2 and 3). These aspects have been experimentally and consistently verified and discussed in our previously published papers.[5−20] The unique feature and combination of R_ϕ and C_ϕ versus E, that is, ($-\varphi$ vs E) or $\Delta(-\varphi)/\Delta E$ and (θ vs E) or $\Delta\theta/\Delta E$, most clearly appear at f_o. The linear relationship and Gaussian profile between ($-\varphi$ vs E) or $\Delta(-\varphi)/\Delta E$ and (θ vs E) or $\Delta\theta/\Delta E$ for f_o imply that only one Frumkin or Langmuir adsorption isotherm is determined on the basis of the relevant experimental results (see Figures 4 to 7). The shape and location of ($-\varphi$ vs E) or $\Delta(-\varphi)/\Delta E$ and (θ vs E) or $\Delta\theta/\Delta E$ for f_o correspond to the interaction parameter (g) and equilibrium constant (K_o) for the Frumkin or the Langmuir adsorption isotherm, respectively. This is another reason why

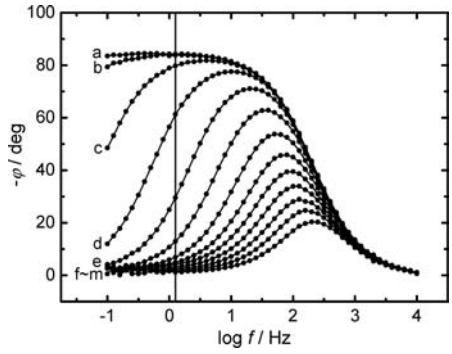

Figure 3. Comparison of the phase-shift curves ($-\varphi$ vs log f) for different potentials (E) on the Pt−Ir alloy in 0.1 M LiOH (D_2O) solution. ●, Measured value. Vertical solid line indicates 1.259 Hz; single sine wave; scan frequency, (10^4 to 0.1) Hz; ac amplitude, 5 mV; dc potential, (a) 0.641 V, (b) 0.691 V, (c) 0.741 V, (d) 0.791 V, (e) 0.841 V, (f) 0.891 V, (g) 0.941 V, (h) 0.991 V, (i) 1.041 V, (j) 1.091 V, (k) 1.141 V, (l) 1.191 V, and (m) 1.241 V versus SHE.

Table 1. Measured Values of the Phase Shift ($-\varphi$) for the Optimum Intermediate Frequency (f_o = 1.259 Hz), the Estimated Fractional Surface Coverage (θ) of Hydroxide (OH), and the Normalized Change Rates ($\Delta(-\varphi)/\Delta E$, $\Delta\theta/\Delta E$) on the Pt−Ir Alloy in 0.1 M LiOH (H_2O) Solution

E/V vs SHE	$-\varphi$/deg	θ ($0 \le \theta \le 1$)	$\Delta(-\varphi)$, $\Delta\theta/\Delta E$
0.641	85.7	≈ 0	≈ 0
0.691	85.3	0.00471	0.03765
0.741	81.8	0.04588	0.32941
0.791	59.2	0.31176	2.12706
0.841	21.9	0.75059	3.51059
0.891	6.8	0.92824	1.42118
0.941	2.7	0.97647	0.38588
0.991	1.2	0.99412	0.14118
1.041	0.7	≈ 1	0.04706

the phase-shift method is the most accurate way to determine adsorption isotherms.

Basic Procedure and Description of the Phase-Shift Method. Figure 2 compares the phase-shift curves ($-\varphi$ vs log f) for different potentials (E) on the Pt−Ir alloy in 0.1 M LiOH (H_2O) solution. The intermediate frequency, that is, a vertical solid line (1.259 Hz) on ($-\varphi$ vs log f) shown in Figure 2, can be set as f_o for ($-\varphi$ vs E) and (θ vs E). At the maximum $-\varphi$ shown in Figure 2a, it appears that the adsorption of OH and superposition of various effects are minimized; that is, $\theta \approx 0$ and E is low. Note that θ ($0 \le \theta \le 1$) depends on E. At the maximum $-\varphi$, when $\theta \approx 0$ and E is low, both $\Delta(-\varphi)/\Delta E$ and $\Delta\theta/\Delta E$ are minimized because of R_ϕ and C_ϕ approaching minimum values. At the minimum $-\varphi$ shown in Figure 2i, it appears that the adsorption of OH and superposition of various effects are maximized or almost saturated; that is, $\theta \approx 1$ and E is high. At the minimum $-\varphi$, when $\theta \approx 1$ and E is high, both $\Delta(-\varphi)/\Delta E$ and $\Delta\theta/\Delta E$ are also minimized because of R_ϕ and C_ϕ approaching minimum values. At the medium $-\varphi$ between parts d and e of Figure 2, it appears that both $\Delta(-\varphi)/\Delta E$ and $\Delta\theta/\Delta E$ are maximized because of R_ϕ and C_ϕ approaching maximum values at $\theta \approx 0.5$ and intermediate E (see Table 1 and Figure 6b).

Figure 3 compares the phase-shift curves ($-\varphi$ vs log f) for different potentials (E) on the Pt−Ir alloy in 0.1 M LiOH (D_2O) solution. Similarly, 1.259 Hz can be set as f_o for ($-\varphi$ vs E) and (θ vs E). At the maximum $-\varphi$ shown in Figure 3a, it appears that the adsorption of (OH, OD) and superposition of various effects are minimized; that is, $\theta \approx 0$ and E is low. As stated above, θ ($0 \le \theta \le 1$) depends on E. At the maximum $-\varphi$, when $\theta \approx 0$ and E is low, both $\Delta(-\varphi)/\Delta E$ and $\Delta\theta/\Delta E$ are

Table 2. Measured Values of the Phase Shift ($-\varphi$) for the Optimum Intermediate Frequency (f_o = 1.259 Hz), the Estimated Fractional Surface Coverage (θ) of Hydroxide and Deuteroxide (OH, OD), and the Normalized Change Rates ($\Delta(-\varphi)/\Delta E$, $\Delta\theta/\Delta E$) on the Pt−Ir Alloy in 0.1 M LiOH (D_2O) Solution

E/V vs SHE	$-\varphi$/deg	θ ($0 \le \theta \le 1$)	$\Delta(-\varphi)$, $\Delta\theta/\Delta E$
0.641	84.3	≈ 0	≈ 0
0.691	83.8	0.00602	0.07220
0.741	79.7	0.05535	0.59206
0.791	61.3	0.27677	2.65704
0.841	29.5	0.65945	4.59206
0.891	12.9	0.85921	2.39711
0.941	6.9	0.93141	0.86643
0.991	4.9	0.95548	0.28881
1.041	4.1	0.96510	0.11552
1.091	3.2	0.97593	0.12996
1.141	2.5	0.98436	0.10108
1.191	1.7	0.99398	0.11552
1.241	1.2	≈ 1	0.07220

minimized because of R_ϕ and C_ϕ approaching minimum values. At the minimum $-\varphi$ shown in Figure 3m, it appears that the adsorption of (OH, OD) and superposition of various effects are maximized or almost saturated; that is, $\theta \approx 1$ and E is high. At the minimum $-\varphi$, when $\theta \approx 1$ and E is high, both $\Delta(-\varphi)/\Delta E$ and $\Delta\theta/\Delta E$ are also minimized because of R_ϕ and C_ϕ approaching minimum values. At the medium $-\varphi$ between parts d and e of Figure 3, it appears that both $\Delta(-\varphi)/\Delta E$ and $\Delta\theta/\Delta E$ are maximized because of R_ϕ and C_ϕ approaching maximum values at $\theta \approx 0.5$ and intermediate E (see Table 2 and Figure 7b).

The procedure and description of the phase-shift method for determining the Frumkin adsorption isotherms of OH and (OH, OD) on the Pt−Ir alloy in 0.1 M LiOH (H_2O) and 0.1 M LiOH (D_2O) solutions are briefly summarized in Tables 1 and 2, respectively. Tables 1 and 2 show the changes of ($-\varphi$ vs E) and (θ vs E) for f_o (= 1.259 Hz) with 50 mV increment changes in positive E on the Pt−Ir alloy in 0.1 M LiOH (H_2O) and 0.1 M LiOH (D_2O) solutions, respectively. The changes of ($-\varphi$ vs E) and (θ vs E) for f_o (= 1.259 Hz) shown in Figures 4 and 5 are illustrated on the basis of the experimental results summarized in Tables 1 and 2, respectively. The changes of ($-\varphi$ vs E) and (θ vs E) for other frequencies (0.1 Hz, 10 Hz, 100 Hz) shown in Figures 4 and 5 are also illustrated through the same procedures summarized in Tables 1 and 2, respectively.

As shown in Figures 2 and 3, $-\varphi$ depends on both f and E, but θ depends on only E. As previously described, the linear relationship and Gaussian profile between ($-\varphi$ vs E) or $\Delta(-\varphi)/\Delta E$ and (θ vs E) or $\Delta\theta/\Delta E$ most clearly appears at f_o. This is the reason why the comparison of ($-\varphi$ vs E) and (θ vs E) for different frequencies shown in Figures 4 and 5 is necessary to determine f_o. Note that ($-\varphi$ vs E) shown in Figures 4a and 5a corresponds to (θ vs E) shown in Figures 4b and 5b, and vice versa, respectively. The difference between ($-\varphi$ vs E) and (θ vs E) for f_o (= 1.259 Hz) and other frequencies (0.1 Hz, 10 Hz, 100 Hz) shown in Figures 4 and 5 does not represent the measurement error but only the frequency response.

Figures 6 and 7 compare the normalized change rates of ($-\varphi$ vs E) and (θ vs E), that is, $\Delta(-\varphi)/\Delta E$ and $\Delta\theta/\Delta E$, for four different frequencies (0.1 Hz, 1.259 Hz, 10 Hz, 100 Hz) on the Pt−Ir alloy in 0.1 M LiOH (H_2O) and 0.1 M LiOH (D_2O) solutions, respectively. The Gaussian profiles shown in Figures 6b and 7b are illustrated on the basis of $\Delta(-\varphi)/\Delta E$ and $\Delta\theta/\Delta E$ for f_o (= 1.259 Hz) summarized in Tables 1 and 2, respectively. Similarly, the Gaussian profiles for other frequencies (0.1 Hz, 10 Hz, 100 Hz) shown in Figures 6 and 7 are obtained through the same procedures summarized in Tables 1 and 2, respectively.

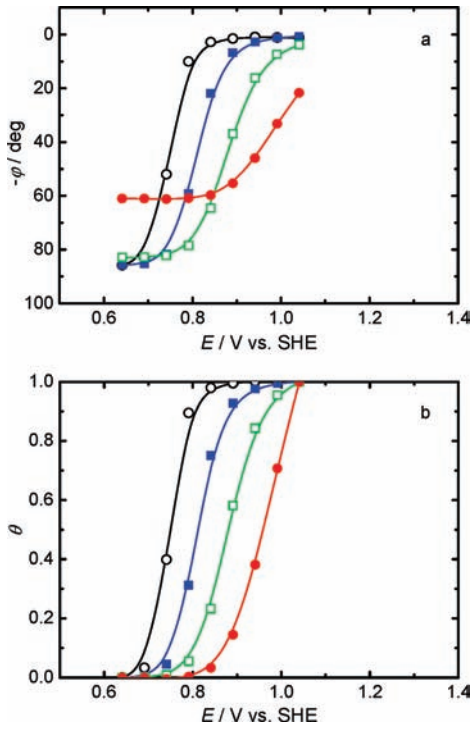

Figure 4. Comparison of (a) the phase-shift profiles ($-\varphi$ vs E) and (b) surface-coverage profiles (θ vs E) for four different frequencies on the Pt−Ir alloy in 0.1 M LiOH (H_2O) solution. Measured or estimated values: ○, 0.1 Hz; ■, 1.259 Hz; □, 10 Hz; ●, 100 Hz. The optimum intermediate frequency (f_o) is 1.259 Hz (■).

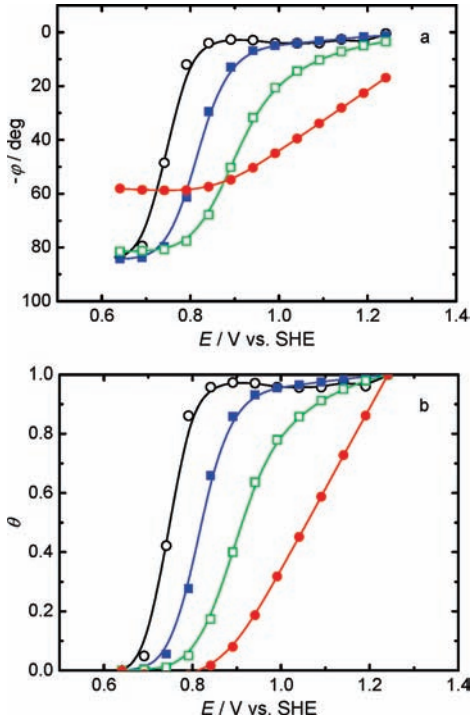

Figure 5. Comparison of (a) the phase-shift profiles ($-\varphi$ vs E) and (b) surface-coverage profiles (θ vs E) for four different frequencies on the Pt−Ir alloy in 0.1 M LiOH (D_2O) solution. Measured or estimated values: ○, 0.1 Hz; ■, 1.259 Hz; □, 10 Hz; ●, 100 Hz. The optimum intermediate frequency (f_o) is 1.259 Hz (■).

In Figures 6b and 7b, $\Delta(-\varphi)/\Delta E$ corresponds to $\Delta\theta/\Delta E$ and vice versa. Both $\Delta(-\varphi)/\Delta E$ and $\Delta\theta/\Delta E$ are maximized at the medium $-\varphi$, when $\theta \approx 0.5$ and E is intermediate, decrease symmetrically with E at other values of θ, and are minimized

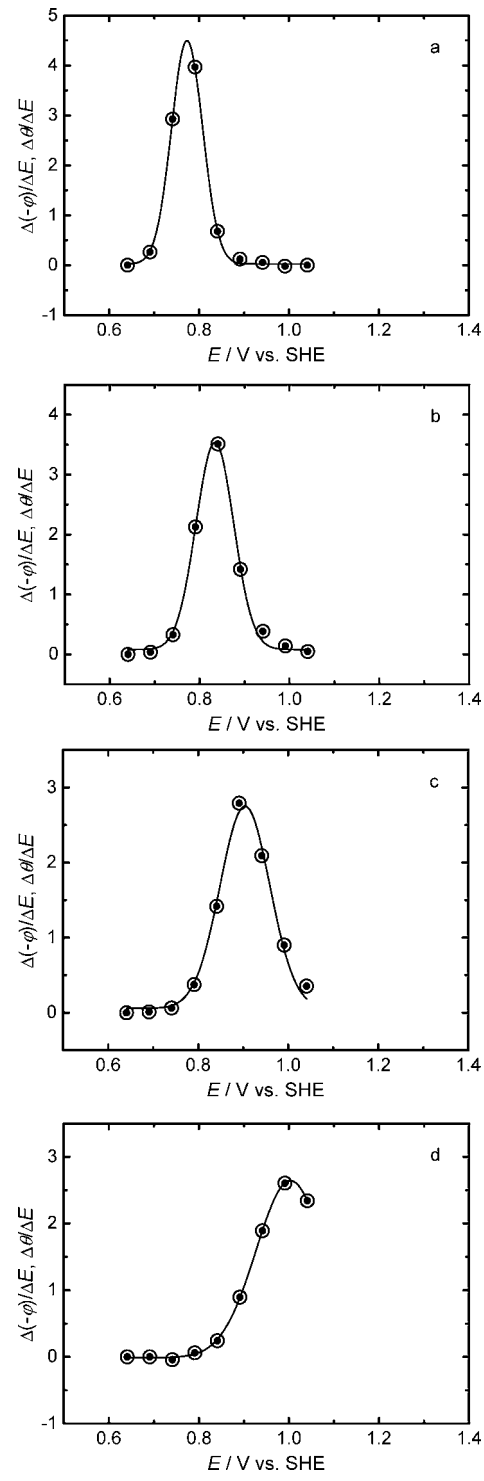

Figure 6. Comparison of the normalized change rates of ($-\varphi$ vs E) and (θ vs E), that is, $\Delta(-\varphi)/\Delta E$ and $\Delta\theta/\Delta E$, for four different frequencies on the Pt−Ir alloy in 0.1 M LiOH (H_2O) solution. —, Fitted Gaussian profile; ○, $\Delta(-\varphi)/\Delta E$; ●, $\Delta\theta/\Delta E$. (a) 0.1 Hz, (b) 1.259 Hz, (c) 10 Hz, and (d) 100 Hz. The optimum intermediate frequency (f_o) is 1.259 Hz.

at the maximum $-\varphi$, when $\theta \approx 0$ and E is low, and the minimum $-\varphi$, when $\theta \approx 1$ and E is high. As previously described, this is a unique feature of the Frumkin and Langmuir adsorption isotherms. The shape and location of ($-\varphi$ vs E) or $\Delta(-\varphi)/\Delta E$ and (θ vs E) or $\Delta\theta/\Delta E$ for f_o correspond to the interaction parameter (g) and equilibrium constant (K_o) for the Frumkin or the Langmuir adsorption isotherm, respectively. The difference between the Gaussian profiles of $\Delta(-\varphi)/\Delta E$ and $\Delta\theta/\Delta E$ for f_o (= 1.259 Hz) and other frequencies (0.1 Hz, 10

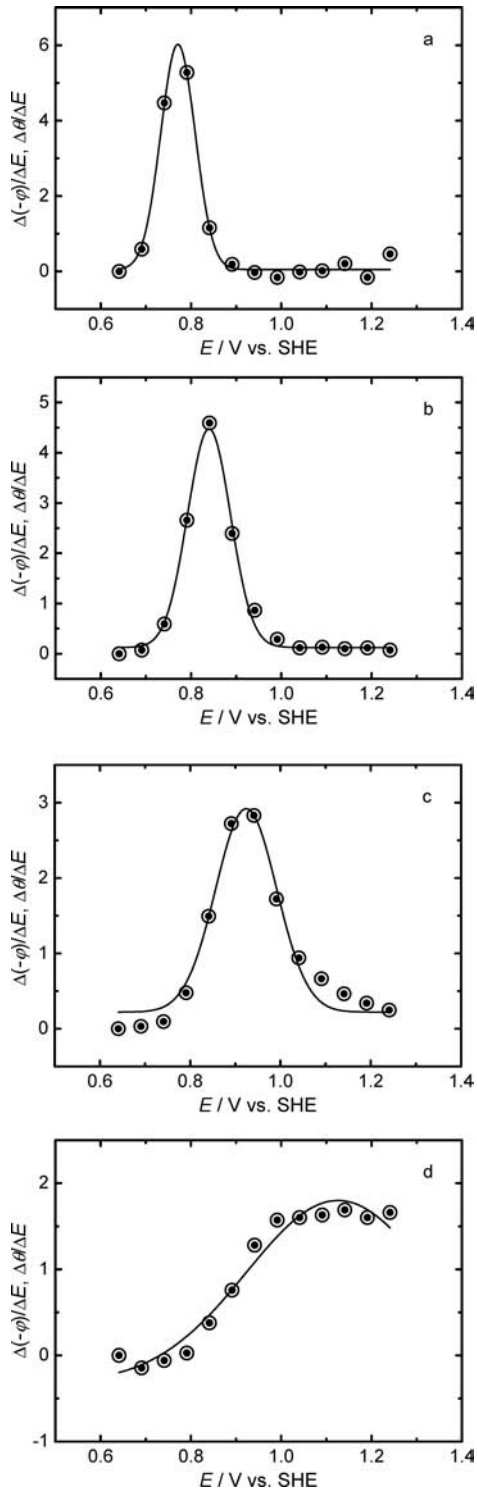

Figure 7. Comparison of the normalized change rates of ($-\varphi$ vs E) and (θ vs E), that is, $\Delta(-\varphi)/\Delta E$ and $\Delta\theta/\Delta E$, for four different frequencies on the Pt−Ir alloy in 0.1 M LiOH (D_2O) solution. —, Fitted Gaussian profile; ○, $\Delta(-\varphi)/\Delta E$; ●, $\Delta\theta/\Delta E$. (a) 0.1 Hz, (b) 1.259 Hz, (c) 10 Hz, and (d) 100 Hz. The optimum intermediate frequency (f_o) is 1.259 Hz.

Hz, 100 Hz) shown in Figures 6 and 7 does not represent the measurement error but only the frequency response.

Finally, one can conclude that the three regions, that is, (maximum $-\varphi$, $\theta \approx 0$, low E), (medium $-\varphi$, $\theta \approx 0.5$, intermediate E), and (minimum $-\varphi$, $\theta \approx 1$, high E), the Gaussian profile, and the corresponding Frumkin or Langmuir adsorption isotherm are readily determined on the basis of ($-\varphi$ vs E) or $\Delta(-\varphi)/\Delta E$ and (θ vs E) or $\Delta\theta/\Delta E$ for f_o (see Tables 1 and 2 and Figures 4 to 7). The linear relationship and Gaussian profile between ($-\varphi$ vs E) or $\Delta(-\varphi)/\Delta E$ and (θ vs E) or $\Delta\theta/\Delta E$ for f_o express the essential nature of the phase-shift method for determining the Frumkin and Langmuir adsorption isotherms. This is not valid and correct for all f and E but only for f_o and a limited range of E.

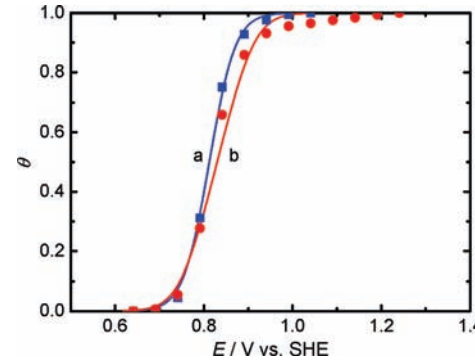

Figure 8. Comparison of the experimental and fitted data for the Frumkin adsorption isotherms (θ vs E) of OH and (OH, OD) on the Pt−Ir alloy in 0.1 M LiOH (H_2O) and 0.1 M LiOH (D_2O) solutions. Experimental data: ■, 0.1 M LiOH (H_2O) solution; ●, 0.1 M LiOH (D_2O) solution. —, Calculated value using eq 4 (Frumkin adsorption isotherm). (a) $K = 5.4 \cdot 10^{-9}$ $\exp(-0.6\theta)$ mol^{-1} for OH and (b) $K = 3.9 \cdot 10^{-9}$ $\exp(-2.7\theta)$ mol^{-1} for (OH, OD).

Frumkin, Langmuir, and Temkin Adsorption Isotherms. The derivation and interpretation of the practical forms of the electrochemical Frumkin, Langmuir, and Temkin adsorption isotherms are described elsewhere.[31−33] The Frumkin adsorption isotherm assumes that the Pt−Ir alloy surface is inhomogeneous or that the lateral interaction effect is not negligible. The Frumkin adsorption isotherm can be expressed as follows[32]

$$[\theta/(1 - \theta)]\exp(g\theta) = K_o C^- [\exp(EF/RT)] \quad (4)$$

$$g = r/RT \quad (5)$$

$$K = K_o \exp(-g\theta) \quad (6)$$

where θ ($0 \le \theta \le 1$) is the fractional surface coverage; g is the interaction parameter for the Frumkin adsorption isotherm; K_o is the equilibrium constant at $g = 0$; C^- is the concentration of ions (OH^-, OD^-) in the bulk solution; E is the positive potential; F is Faraday's constant; R is the gas constant; T is the absolute temperature; r is the rate of change of the standard Gibbs energy of adsorption with θ; and K is the equilibrium constant. The dimension of K is described elsewhere.[34] Note that $g = 0$ in eqs 4 to 6, which implies the Langmuir adsorption isotherm. For the Langmuir adsorption isotherm, when $g = 0$, the inhomogeneous and lateral interaction effects on the adsorption are negligible.

Figures 8a and b show the Frumkin adsorption isotherms of OH and (OH, OD) on the Pt−Ir alloy in 0.1 M LiOH (H_2O) and 0.1 M LiOH (D_2O) solutions, respectively. These Frumkin adsorption isotherms are numerically calculated using eq 4. The Frumkin adsorption isotherms shown in Figures 8a and b are illustrated on the basis of the experimental results summarized in Tables 1 and 2, respectively. Figure 8a shows the Frumkin adsorption isotherm corresponding to $g = 0.6$ for $K_o = 5.4 \cdot 10^{-9}$ mol^{-1}, that is, $K = 5.4 \cdot 10^{-9}$ $\exp(-0.6\theta)$ mol^{-1}. Using eq 5, r is 1.5 $kJ \cdot mol^{-1}$. Similarly, Figure 8b shows the Frumkin adsorption isotherm corresponding to $g = 2.7$ for $K_o = 3.9 \cdot 10^{-9}$

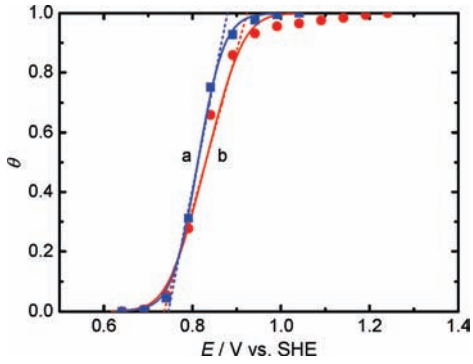

Figure 9. Comparison of the experimental and fitted data for the Frumkin and Temkin adsorption isotherms (θ vs E) of OH and (OH, OD) on the Pt−Ir alloy in 0.1 M LiOH (H_2O) and 0.1 M LiOH (D_2O) solutions. Experimental data: ■, 0.1 M LiOH (H_2O) solution; ●, 0.1 M LiOH (D_2O) solution. —, Calculated value using eq 4 (Frumkin adsorption isotherm). ----, Calculated value using eq 7 (Temkin adsorption isotherm) and the correlation constants. (a) $K = 5.4 \cdot 10^{-8} \exp(-5.2\theta)$ mol^{-1} for OH and (b) $K = 3.9 \cdot 10^{-8} \exp(-7.3\theta)$ mol^{-1} for (OH, OD). Note that the Temkin adsorption isotherms are only valid and effective at $0.2 < \theta < 0.8$.

mol^{-1}, that is, $K = 3.9 \cdot 10^{-9} \exp(-2.7\theta)$ mol^{-1}. Using eq 5, r is 6.7 kJ·mol^{-1}. Figure 8b also shows that the OD effect on the Frumkin adsorption isotherm of (OH, OD) increases with increasing E and θ. The applicability of the Frumkin adsorption isotherm of (OH, OD) is not accurate when $0.94 < \theta$.

In contrast to a lateral attraction ($g < 0$) interaction between the adsorbed H species on the Pt, Ir, and Pt−Ir alloy,[15,17,20] a lateral repulsion ($g > 0$) interaction between the adsorbed OH or (OH, OD) species appears. This implies that the duality of the lateral attraction and repulsion interactions between the adsorbed OH or (OH, OD) species on the Pt, Ir, and Pt−Ir alloys in alkaline H_2O and D_2O solutions does not appear.

By comparing Figure 8a with Figure 8b, one can interpret that the difference between the Frumkin adsorption isotherms of OH and (OH, OD) is not negligible. This difference increases with increasing E and θ. Note that this is attributed to the OD^- in 0.1 M LiOH (D_2O) solution. In other words, the OD effect on the adsorption of (OH, OD) on the Pt−Ir alloy in 0.1 M LiOH (D_2O) solution increases with increasing E and θ. This OD effect is not negligible, especially, when E is high and $\theta \approx 1$. Depending on θ, that is, $0 \le \theta \le 1$, the value of K for OH is approximately 1.4 to 11.5 times greater than that for (OH, OD). Both the values of K for OH and (OH, OD) decrease with increasing E and θ. As stated above, this is attributed to the lateral repulsion ($g > 0$) interaction between the adsorbed OH or (OH, OD) species.

At intermediate values of θ, that is, $0.2 < \theta < 0.8$, the pre-exponential term, $[\theta/(1 - \theta)]$, varies little with θ compared to the variation of the exponential term, $\exp(g\theta)$ (see eq 4). Under the approximate conditions, the Temkin adsorption isotherm can be simply derived from the Frumkin adsorption isotherm. The Temkin adsorption isotherm can be expressed as follows[32]

$$\exp(g\theta) = K_o C^- [\exp(EF/RT)] \quad (7)$$

Figures 9a and b show the Temkin adsorption isotherms correlating with the Frumkin adsorption isotherms shown in Figures 8a and b, respectively. These Temkin adsorption isotherms are numerically calculated using eq 7 and the correlation constants.[14−20] The Temkin adsorption isotherm, $g = 5.2$ for $K_o = 5.4 \cdot 10^{-8}$ mol^{-1}, that is, $K = 5.4 \cdot 10^{-8} \exp(-5.2\theta)$ mol^{-1}, shown in Figure 9a is applicable to the adsorption of OH. Using eq 5, r is 12.9 kJ·mol^{-1}. Similarly, the Temkin adsorption isotherm, $g = 7.3$ for $K_o = 3.9 \cdot 10^{-8}$ mol^{-1}, that is, $K = 3.9 \cdot 10^{-8} \exp(-7.3\theta)$ mol^{-1}, shown in Figure 9b is applicable to the adsorption of (OH, OD). Using eq 5, r is 18.1 kJ·mol^{-1}.

A lateral repulsion ($g > 0$) interaction between the adsorbed OH or (OH, OD) species appears at $0.2 < \theta < 0.8$. Depending on θ, that is, $0.2 < \theta < 0.8$, the value of K for OH is approximately 2.1−7.6 times greater than that for (OH, OD). Note that the Temkin adsorption isotherms are only valid and effective at $0.2 < \theta < 0.8$. The applicability and determination of the Temkin adsorption isotherm are described elsewhere.[20]

Correlation Constants between the Adsorption Isotherms. As previously described, the Frumkin, Langmuir, and Temkin adsorption conditions are different from each other. Only one Frumkin or Langmuir adsorption isotherm is determined on the basis of the relevant experimental results. At $0.2 < \theta < 0.8$, the Temkin adsorption isotherm correlating with the Frumkin or Langmuir adsorption isotherm, and vice versa, is readily determined using the correlation constants. The two different adsorption isotherms, that is, the Temkin and Frumkin or Langmuir adsorption isotherms, appear to fit the same data regardless of their adsorption conditions.

In this work, one can also confirm that the values of g and K_o for the Temkin adsorption isotherms are approximately 4.6 and 10 times greater than those for the correlating Frumkin adsorption isotherms, respectively. These numbers (ca. 4.6 and 10 times) can be taken as correlation constants between the Temkin and Frumkin or Langmuir adsorption isotherms. The unique feature of the Temkin and Frumkin or Langmuir adsorption isotherms has been experimentally and consistently verified using the phase-shift method and correlation constants.[14,15,18−20]

Standard Gibbs Energy of Adsorption. The standard Gibbs energy of OH or (OH, OD) is given by the difference between the standard molar Gibbs energy of OH or (OH, OD) and that of a number of H_2O or D_2O molecules on the adsorption sites of the Pt−Ir alloy surface. Under the Frumkin adsorption conditions, the relation between the equilibrium constant (K)

Table 3. Comparison of the Standard Gibbs Energies (ΔG_θ^0) of Hydroxide (OH), Hydroxide and Deuteroxide (OH, OD), Hydrogen (H), and the Equilibrium Constants (K) for the Frumkin Adsorption Isotherms on the Pt, Ir, and Pt−Ir Alloys in Solutions

metal (alloy)/solution	adsorbate	ΔG_θ^0 / kJ·mol^{-1}	K / mol^{-1}	ref
Pt−Ir alloy[a]/0.1 M LiOH (H_2O)	OH	$47.2 \le \Delta G_\theta^0 \le 48.6$	$5.4 \cdot 10^{-9} \exp(-0.6\theta)$	this work
Pt−Ir alloy[b]/0.1 M LiOH (D_2O)	OH, OD	$48.0 \le \Delta G_\theta^0 \le 54.7$	$3.9 \cdot 10^{-9} \exp(-2.7\theta)$	this work
Pt−Ir alloy[c]/0.1 M KOH (H_2O)	OH	$53.2 \le \Delta G_\theta^0 \le 57.7$	$4.7 \cdot 10^{-10} \exp(-1.8\theta)$	15
Pt−Ir alloy[d]/0.5 M H_2SO_4 (H_2O)	H	$25.7 \ge \Delta G_\theta^0 \ge 19.5$	$3.1 \cdot 10^{-5} \exp(2.5\theta)$	15
Pt[e]/0.1 M KOH (H_2O)	H	$22.4 \ge \Delta G_\theta^0 \ge 16.5$	$1.2 \cdot 10^{-4} \exp(2.4\theta)$	20
Ir[f]/0.1 M KOH (H_2O)	H	$23.0 \ge \Delta G_\theta^0 \ge 17.1$	$9.4 \cdot 10^{-5} \exp(2.4\theta)$	20

[a] Pt−Ir alloy (90:10 % (by weight)). [b] Pt−Ir alloy (90:10 % (by weight)). [c] Pt−Ir alloy (70:30 % (by weight)). [d] Pt−Ir alloy (70:30 % (by weight)). [e] Pt (purity: 99.9985 %). [f] Ir (purity: 99.8 %). Note that the Frumkin adsorption isotherms are valid and effective at $0 \le \theta \le 1$.

Table 4. Comparison of the Standard Gibbs Energies (ΔG_θ^0) of Hydroxide (OH), Hydroxide and Deuteroxide (OH, OD), Hydrogen (H), and the Equilibrium Constants (K) for the Temkin Adsorption Isotherms on the Pt, Ir, and Pt−Ir Alloys in Solutions

		ΔG_θ^0	K	
metal (alloy)/solution	adsorbate	kJ·mol^{-1}	mol^{-1}	ref
Pt−Ir alloy[a]/0.1 M LiOH (H_2O)	OH	$44.0 < \Delta G_\theta^0 < 51.8$	$5.4\cdot10^{-8}\exp(-5.2\theta)$	this work
Pt−Ir alloy[b]/0.1 M LiOH (D_2O)	OH, OD	$45.9 < \Delta G_\theta^0 < 56.8$	$3.9\cdot10^{-8}\exp(-7.3\theta)$	this work
Pt−Ir alloy[c]/0.1 M KOH (H_2O)	OH	$50.7 < \Delta G_\theta^0 < 60.2$	$4.7\cdot10^{-9}\exp(-6.4\theta)$	15
Pt−Ir alloy[d]/0.5 M H_2SO_4 (H_2O)	H	$21.1 < \Delta G_\theta^0 < 24.2$	$3.1\cdot10^{-4}\exp(-2.1\theta)$	15
Pt[e]/0.1 M KOH (H_2O)	H	$17.8 < \Delta G_\theta^0 < 21.0$	$1.2\cdot10^{-3}\exp(-2.2\theta)$	20
Ir[f]/0.1 M KOH (H_2O)	H	$18.3 < \Delta G_\theta^0 < 21.7$	$9.4\cdot10^{-4}\exp(-2.2\theta)$	20

[a] Pt−Ir alloy (90:10 % (by weight)). [b] Pt−Ir alloy (90:10 % (by weight)). [c] Pt−Ir alloy (70:30 % (by weight)). [d] Pt−Ir alloy (70:30 % (by weight)). [e] Pt (purity: 99.9985 %). [f] Ir (purity: 99.8 %). Note that the Temkin adsorption isotherms are only valid and effective at $0.2 < \theta < 0.8$.

for OH or (OH, OD) and the standard Gibbs energy (ΔG_θ^0) of OH or (OH, OD) is given as follows[32]

$$2.3RT \log K = -\Delta G_\theta^{\ 0} \tag{8}$$

On the Pt−Ir alloy in 0.1 M LiOH (H_2O) solution, using eqs 6 and 8, ΔG_θ^0 of OH is ($47.2 \le \Delta G_\theta^0 \le 48.6$) kJ·mol^{-1} for $K = 5.4\cdot10^{-9}\exp(-0.6\theta)$ mol^{-1} and $0 \le \theta \le 1$. This result implies a decrease of ΔG_θ^0 of OH with θ ($0 \le \theta \le 1$). Note that ΔG_θ^0 is a negative number. The standard Gibbs energies (ΔG_θ^0) of OH, (OH, OD), H, and the equilibrium constants (K) for the Frumkin and Temkin adsorption isotherms on the Pt, Ir, and Pt−Ir alloys in solutions are summarized in Tables 3 and 4, respectively.

Conclusions

On the Pt−Ir alloy in 0.1 M LiOH (H_2O) solution, the Frumkin and Temkin adsorption isotherms (θ vs E), equilibrium constants ($K = 5.4\cdot10^{-9}\exp(-0.6\theta)$ mol^{-1} for the Frumkin and $K = 5.4\cdot10^{-8}\exp(-5.2\theta)$ mol^{-1} for the Temkin adsorption isotherm), interaction parameters ($g = 0.6$ for the Frumkin and $g = 5.2$ for the Temkin adsorption isotherm), rates of change of the standard Gibbs energies ($r = 1.5$ kJ·mol^{-1} for $g = 0.6$ and $r = 12.9$ kJ·mol^{-1} for $g = 5.2$) of OH with θ, and standard Gibbs energies [($47.2 \le \Delta G_\theta^0 \le 48.6$) kJ·mol^{-1} for $K = 5.4\cdot10^{-9}\exp(-0.6\theta)$ mol^{-1} and $0 \le \theta \le 1$ and ($44.0 < \Delta G_\theta^0 < 51.8$) kJ·mol^{-1} for $K = 5.4\cdot10^{-8}\exp(-5.2\theta)$ mol^{-1} and $0.2 < \theta < 0.8$] of OH are determined using the phase-shift method and correlation constants.

On the Pt−Ir alloy in 0.1 M LiOH (D_2O) solution, the Frumkin and Temkin adsorption isotherms (θ vs E), equilibrium constants ($K = 3.9\cdot10^{-9}\exp(-2.7\theta)$ mol^{-1} for the Frumkin and $K = 3.9\cdot10^{-8}\exp(-7.3\theta)$ mol^{-1} for the Temkin adsorption isotherm), interaction parameters ($g = 2.7$ for the Frumkin and $g = 7.3$ for the Temkin adsorption isotherm), rates of change of the standard Gibbs energies ($r = 6.7$ kJ·mol^{-1} for $g = 2.7$ and $r = 18.1$ kJ·mol^{-1} for $g = 7.3$) of (OH, OD) with θ, and standard Gibbs energies [($48.0 \le \Delta G_\theta^0 \le 54.7$) kJ·mol^{-1} for $K = 3.9\cdot10^{-9}\exp(-2.7\theta)$ mol^{-1} and $0 \le \theta \le 1$ and ($45.9 < \Delta G_\theta^0 < 56.8$) kJ·mol^{-1} for $K = 3.9\cdot10^{-8}\exp(-7.3\theta)$ mol^{-1} and $0.2 < \theta < 0.8$] of (OH, OD) are determined using the phase-shift method and correlation constants.

Depending on θ ($0 \le \theta \le 1$), the value of K for OH is approximately 1.4 to 11.5 times greater than that for (OH, OD). The OD effect on the adsorption of (OH, OD) on the Pt−Ir alloy in 0.1 M LiOH (D_2O) solution is not negligible, especially when E is high and $\theta \approx 1$. Both the values of K for OH and (OH, OD) decrease with increasing E and θ. A lateral repulsion ($g > 0$) interaction between the adsorbed OH or (OH, OD) species appears.

The phase-shift method and correlation constants are the most accurate, useful, and effective ways to determine the Frumkin, Langmuir, and Temkin adsorption isotherms and related electrode kinetic and thermodynamic parameters of noble and highly corrosion-resistant metals (alloys) in H_2O and D_2O solutions.

Supporting Information Available:

Comparisons of the measured and calculated values of the phase shift ($-\varphi$) for the optimum intermediate frequency ($f_o = 1.259$ Hz) on the Pt−Ir alloy in 0.1 M LiOH (H_2O) and 0.1 M LiOH (D_2O) solutions are shown in Supplementary Tables 1 and 2, respectively. This material is available free of charge via the Internet at http://pubs.acs.org.

Literature Cited

(1) Gileadi, E.; Kirowa-Eisner, E.; Penciner, J. *Interfacial electrochemistry*; Addison-Wesley: Reading, MA, 1975.
(2) Gileadi, E. *Electrode kinetics*; VCH: New York, 1993.
(3) Bockris, JO'M.; Khan, S. U. M. *Surface electrochemistry*; Plenum Press: New York, 1993.
(4) Gileadi, E. *Electrosorption: Adsorption in electrochemistry*; Gileadi, E., Ed.; Plenum Press: New York, 1967; pp 1−18.
(5) Chun, J. H.; Ra, K. H. The phase-shift method for the Frumkin adsorption isotherms at the Pd/H_2SO_4 and KOH solution interfaces. *J. Electrochem. Soc.* **1998**, *145*, 3794–3798.
(6) Chun, J. H.; Ra, K. H.; Kim, N. Y. The Langmuir adsorption isotherms of electroadsorbed hydrogens for the cathodic hydrogen evolution reactions at the Pt(100)/H_2SO_4 and LiOH aqueous electrolyte interfaces. *Int. J. Hydrogen Energy* **2001**, *26*, 941–948.
(7) Chun, J. H.; Ra, K. H.; Kim, N. Y. Qualitative analysis of the Frumkin adsorption isotherm of the over-potentially deposited hydrogen at the poly-Ni/KOH aqueous electrolyte interface using the phase-shift method. *J. Electrochem. Soc.* **2002**, *149*, E325−330.
(8) Chun, J. H.; Ra, K. H.; Kim, N. Y. Langmuir adsorption isotherms of over-potentially deposited hydrogen at poly-Au and Rh/H_2SO_4 aqueous electrolyte interfaces: Qualitative analysis using the phase-shift method. *J. Electrochem. Soc.* **2003**, *150*, E207−217.
(9) Chun, J. H. Methods for estimating adsorption isotherms in electrochemical systems. U.S. Patent, 2003, 6613218.
(10) Chun, J. H.; Jeon, S. K.; Kim, B. K.; Chun, J. Y. Determination of the Langmuir adsorption isotherms of under- and over-potentially deposited hydrogen for the cathodic H_2 evolution reaction at poly-Ir/aqueous electrolyte interfaces using the phase-shift method. *Int. J. Hydrogen Energy* **2005**, *30*, 247–259.
(11) Chun, J. H.; Jeon, S. K.; Ra, K. H.; Chun, J. Y. The phase-shift method for determining Langmuir adsorption isotherms of over-potentially deposited hydrogen for the cathodic H_2 evolution reaction at poly-Re/aqueous electrolyte interfaces. *Int. J. Hydrogen Energy* **2005**, *30*, 485–499.
(12) Chun, J. H.; Jeon, S. K.; Kim, N. Y.; Chun, J. Y. The phase-shift method for determining Langmuir and Temkin adsorption isotherms of over-potentially deposited hydrogen for the cathodic H_2 evolution reaction at the poly-Pt/H_2SO_4 aqueous electrolyte interface. *Int. J. Hydrogen Energy* **2005**, *30*, 1423–1436.
(13) Chun, J. H.; Kim, N. Y. The phase-shift method for determining adsorption isotherms of hydrogen in electrochemical systems. *Int. J. Hydrogen Energy* **2006**, *31*, 277–283.
(14) Chun, J. H.; Jeon, S. K.; Chun, J. Y. The phase-shift method and correlation constants for determining adsorption isotherms of hydrogen at a palladium electrode interface. *Int. J. Hydrogen Energy* **2007**, *32*, 1982–1990.

(15) Chun, J. H.; Kim, N. Y.; Chun, J. Y. Determination of adsorption isotherms of hydrogen and hydroxide at Pt-Ir alloy electrode interfaces using the phase-shift method and correlation constants. *Int. J. Hydrogen Energy* **2008**, *33*, 762–774.
(16) Chun, J. Y.; Chun, J. H. Correction and supplement to the determination of the optimum intermediate frequency for the phase-shift method [Chun et al., Int. J. Hydrogen Energy 30 (2005) 247−259, 1423−1436]. *Int. J. Hydrogen Energy* **2008**, *33*, 4962–4965.
(17) Chun, J. Y.; Chun, J. H. A negative value of the interaction parameter for over-potentially deposited hydrogen at Pt, Ir, and Pt-Ir alloy electrode interfaces. *Electrochem. Commun.* **2009**, *11*, 744–747.
(18) Chun, J. Y.; Chun, J. H. Determination of adsorption isotherms of hydrogen on titanium in sulfuric acid solution using the phase-shift method and correlation constants. *J. Chem. Eng. Data* **2009**, *54*, 1236–1243.
(19) Chun, J. H.; Chun, J. Y. Determination of adsorption isotherms of hydrogen on zirconium in sulfuric acid solution using the phase-shift method and correlation constants. *J. Korean Electrochem. Soc.* **2009**, *12*, 26–33.
(20) Chun, J.; Lee, J.; Chun, J. H. Determination of adsorption isotherms of overpotentially deposited hydrogen on platinum and iridium in KOH aqueous solution using the phase-shift method and correlation constants. *J. Chem. Eng. Data* **2010**, *55*, 2363–2372.
(21) Kvastek, K.; Horvat-Radosevic, V. Comment on: Langmuir adsorption isotherms of over-potentially deposited hydrogen at poly-Au and Rh/H_2SO_4 aqueous electrolyte interfaces; Qualitative analysis using the phase-shift method *J. Electrochem. Soc.* **2003**, *150*, E207−217. *J. Electrochem. Soc.* **2004**, *151*, L9−10.
(22) Lasia, A. Comments on: The phase-shift method for determining Langmuir adsorption isotherms of over-potentially deposited hydrogen for the cathodic H_2 evolution reaction at poly-Re/aqueous electrolyte interfaces. *Int. J. Hydrogen Energy* **2005**, *30*, 485−499; *Int. J. Hydrogen Energy* **2005**, *30*, 913−917.
(23) Horvat-Radosevic, V.; Kvastek, K. Pitfalls of the phase-shift method for determining adsorption isotherms. *Electrochem. Commun.* **2009**, *11*, 1460–1463.
(24) Chun, J. H.; Ra, K. H.; Kim, N. Y. Response to comment on: Langmuir adsorption isotherms of over-potentially deposited hydrogen at poly-Au and Rh/H_2SO_4 aqueous electrolyte interfaces; Qualitative analysis using the phase-shift method. *J. Electrochem. Soc.* **2003**, *150*, E207−217; *J. Electrochem. Soc.* **2004**, *151*, L11−13.
(25) Chun, J. H.; Jeon, S. K.; Kim, N. Y.; Chun, J. Y. Response to comments on: The phase-shift method for determining Langmuir adsorption isotherms of over-potentially deposited hydrogen for the cathodic H_2 evolution reaction at poly-Re/aqueous electrolyte interfaces. *Int. J. Hydrogen Energy* **2005**, *30*, 485−499; *Int. J. Hydrogen Energy* **2005**, *30*, 919−928.
(26) In our e-mail communications, Horvat-Radosevic and Kvastek admitted that all of their objections to the phase-shift method in ref 23 were confused and misunderstood. The exact same confusion and misunderstanding about the phase-shift method also appear in refs 21 and 22. They still do not understand and accept the phase-shift method itself without reliable simulation or experimental data.
(27) Gileadi, E.; Kirowa-Eisner, E.; Penciner, J. *Interfacial electrochemistry*; Addison-Wesley: Reading, MA, 1975; pp 6, 72−73.
(28) Gileadi, E.; Kirowa-Eisner, E.; Penciner, J. *Interfacial electrochemistry*; Addison-Wesley: Reading, MA, 1975; pp 86−93.
(29) Gileadi, E. *Electrode kinetics*; VCH: New York, 1993; pp 291−303.
(30) Harrington, D. A.; Conway, B. E. AC impedance of faradaic reactions involving electrosorbed intermediates-I. Kinetic theory. *Electrochim. Acta* **1987**, *32*, 1703–1712.
(31) Gileadi, E.; Kirowa-Eisner, E.; Penciner, J. *Interfacial electrochemistry*; Addison-Wesley: Reading, MA, 1975; pp 82−86.
(32) Gileadi, E. *Electrode kinetics*; VCH: New York, 1993; pp 261−280.
(33) Bockris, JO'M.; Reddy, A. K. N.; Gamboa-Aldeco, M. *Modern electrochemistry*; 2nd ed.; Kluwer Academic/Plenum Press: New York, 2000; Vol. 2A, pp 1193−1197.
(34) Oxtoby, D. W.; Gillis, H. P.; Nachtrieb, N. H. *Principles of modern chemistry*, 5th ed.; Thomson Learning Inc.: New York, 2002; p 446.

Received for review April 5, 2010. Accepted July 17, 2010. This work was supported by the Research Grant of Kwangwoon University in 2010.

JE100328D